# Supramolecular Staircase via Self-Assembly of Disklike Molecules at the Solid−Liquid Interface

**Paolo Samorí,[†] Andreas Fechtenkötter,[‡] Frank Jäckel,[†] Thilo Böhme,[†] Klaus Müllen,*[,‡] and Jürgen P. Rabe*[,†]**

*Contribution from the Department of Physics, Humboldt University Berlin, Invalidenstrasse 110, 10115 Berlin, Germany, and MPI for Polymer Research, Ackermannweg 10, 55128 Mainz, Germany*

*Received May 7, 2001*

**Abstract:** A series of soluble hexabenzocoronene (HBC) derivatives with pendant optically active (*S*)-3,7-dimethyloctanyl and (*R*,*S*)-3,7-dimethyloctanyl (mixture of stereoisomers) hydrocarbon side chains with and without a phenylene spacer were assembled into differently ordered arrays at the interface between a solution and the basal plane of highly oriented pyrolytic graphite (HOPG). Molecularly resolved scanning tunneling microscopy (STM) images revealed that all derivatives self-assemble into oriented crystals in quasi-two dimensions. However, while for the alkyl-substituted HBCs (**1**,**4**) all of the single aromatic cores within a monolayer exhibit the same contrast in the STM, the single aromatic cores with a phenylene group between the alkyl side chains and the aromatic core (**2a**,**2b**,**3)** exhibit different contrasts within a monolayer. For the disks carrying racemic branched or *n*-alkyl side chains **(2b**,**3)** a random distribution of the two different contrasts within the 2D-crystal is observed, while the optically active phenylene-alkyl-substituted HBC (**2a**) exhibits a periodical distribution of three contrasts within the monolayer. We attribute the different contrasts of the aromatic cores in the presence of the phenylene groups to a loss of the planarity of the whole molecule and different conformations, which allow the conjugated disks to attain different equilibrium positions above the surface of HOPG. In the case of the optically active side chains a regular superstructure with three distinctly different positions such as in a staircase is attained. The self-assembly processes are governed by the interplay of intramolecular as well as intermolecular and interfacial interactions. In the present case, the interactions may induce both the molecules to acquire well distinct positions along the *z* axis and to adopt different conformations. The reported results open new avenues of exploration. For instance, the different couplings of conjugated molecules with the substrate at different separations can be investigated by means of scanning tunneling spectroscopy (STS). Furthermore, experiments on the STM tip-induced switching of single molecules embedded in a monolayer appear feasible.

## Introduction

The self-assembly of nanometer-sized building blocks into targeted molecular architectures at surfaces represents one of the major goals of supramolecular chemistry and material science, given the perspective of the potential applications of these systems in nanotechnology, for example, for molecular information storage devices or functional surfaces.[1] This requires an accurate control of the molecular arrangements over a wide range of length scales, spanning from micrometers down to the molecular size. Noncovalent intermolecular forces have been used to engineer highly ordered three-dimensional (macro)-molecular architectures where the single building blocks are held together by specific interactions, such as metal−ligand bonding,[2] hydrogen bonding[3] or $\pi-\pi$ stacking.[4] On the other hand, the self-assembly at the solid−liquid interface has been successfully used to control the molecular arrangement in two dimensions.[3b,5]

Polycyclic aromatic hydrocarbons (PAHs), which can be regarded as two-dimensional subsections of graphite, are well-defined nanoobjects[6−18] with interesting electronic properties.[7,8,10,14,16] During the last few years, soluble derivatives, namely, hexa-*peri*-hexabenzocoronenes (HBCs), and larger analogues have been synthesized. From a synthetic point of view, they are extremely versatile compounds that are able to bear different chemical functionalities in their periphery.[10−18]

Scanning tunneling microscopy (STM) is a technique which allows the investigation of physisorbed layers of PAHs both at

* Corresponding authors. Prof. Dr. K. Müllen: e-mail: muellen@mpip-mainz.mpg.de; fax: +49-6131-379350. Prof. Dr. J. P. Rabe: e-mail rabe@physik.hu-berlin.de; fax: +49-30-20937632.

[†] Humboldt University Berlin.

[‡] MPI for Polymer Research.

(1) (a) Lehn, J.-M. *Supramolecular Chemistry: Concepts and Perspectives*; VCH: Weinheim, 1995. (b) Philp, D.; Stoddart, J. F. *Angew. Chem.* **1996**, *108*, 1242−1286; *Angew. Chem., Int. Ed. Engl.* **1996**, *35*, 1155−1196.

(2) (a) Semenov, A.; Spatz, J. P.; Möller, M.; Lehn, J.-M.; Sell, B.; Schubert, D.; Weidl, C. H.; Schubert, U. S. *Angew. Chem.* **1999**, *111*, 2701−2705; *Angew. Chem., Int. Ed. Engl.* **1999**, *38*, 2547−2550. (b) Guo, S.; Konopny, L.; Popovitz-Biro, R.; Cohen, H.; Porteanu, H.; Lifshitz, E.; Lahav, M. *J. Am. Chem. Soc.* **1999**, *121*, 9589−9598. (c) Kurth, D. G.; Lehmann, P.; Schütte, M. *Proc. Natl. Acad. Sci. U.S.A.* **2000**, *97*, 5704−5707.

(3) (a) Desiraju, G. R. *Angew. Chem.* **1995**, *107*, 2541−2558; *Angew. Chem., Int. Ed. Engl.* **1995**, *34*, 2311−2327. (b) Gottarelli, G.; Masiero, S.; Mezzina, E.; Pieraccini, S.; Rabe, J. P.; Samorí, P.; Spada, G. P. *Chem. Eur. J.* **2000**, *6*, 3242−3248. (c) Hirschberg, J. H. K. K.; Brunsveld, L.; Ramzi, A.; Vekemans, J. A. J. M.; Sijbesma, R. P.; Meijer, E. W. *Nature* **2000**, *407*, 167−170. (d) Bisson, A. P.; Carver, F. J.; Eggleston D. S.; Haltiwanger, R. C.; Hunter, C. A.; Livingstone, D. L.; McCabe, J. F.; Rotger, C.; Rowan, A. E. *J. Am. Chem. Soc.* **2000**, *122*, 8856−8868. (e) Böhringer, M.; Schneider, W.-D.; Berndt, R. *Angew. Chem.* **2000**, *112*, 821−825; *Angew. Chem., Int. Ed.* **2000**, *39*, 792−795.

(4) Engelkamp, H.; Middelbeek, S.; Nolte, R. J. M. *Science* **1999**, *284*, 785−788.

10.1021/ja0111380 CCC: $20.00 
Published on Web 10/26/2001

the graphite−solution interface[8−10,14,17] and in dry thin films on conductive substrates[18] with molecular resolution. The first type of PAH which has been explored were triphenylene derivatives,[8,9] which possess 18 carbon atoms in the aromatic core. Following the recent achievements in the synthesis of larger and larger PAHs, the packing at surfaces of compounds with 42[10,17,18] and 60 carbons[14] in the conjugated core has been also studied. These systems have been found to form two-dimensional crystals where the disklike molecules lie flat on the basal plane of the conductive substrate. Recently, an STM investigation of self-assembled monolayers of a series of triphenylene derivatives with increasing lengths of the alkyl side substituents has been reported which revealed different periodically distributed contrasts of the conjugated disks: the observed structures have been explained with a frustrated Ising net model.[9]

In a previous report it has been shown that HBC−$C_{12}$ (**4**) (Figure 1) can crystallize in monolayers at the solution−graphite interface with all conjugated cores lying equally flat on the basal plane of the HOPG.[10] STM and STS have been used to study the molecular structure and electronic properties of the monolayer on the molecular scale. In the latter type of analysis, a diode like electrical behavior of the conjugated HBC core in the gap tip-substrate has been observed.[10]

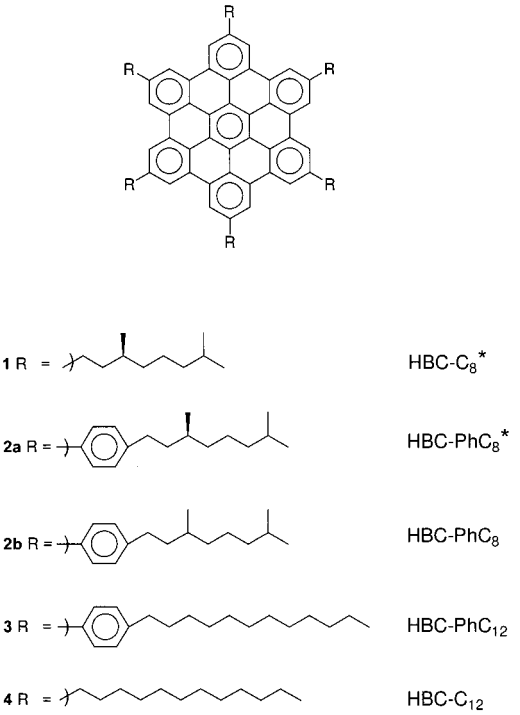


**Figure 1.** Chemical formulas.

With the aim of extending the molecular order of the physisorbed layers to the third dimension (*z* axis) in the region near the substrate surface, we have investigated HBC derivatives symmetrically functionalized in the peripheral positions with more bulky side chains, which, due to steric hindrances could force neighboring HBCs to acquire different positions along the *z* axis.

We report here a submolecularly resolved STM investigation of the self-assembly of different enantiomerically pure (*S*) or (*R*,*S*) hydrocarbon-substituted HBCs with and without a phenylene spacer (Figure 1) into monolayers highly ordered at the graphite−solution interface.

Compound **1** is bearing alkyl side chains exhibiting a chiral methyl function in the 3′-position and a racemic one in the 7′-position. In compound **2a** a phenylene has been introduced between the HBC core and the enantiomerically pure aliphatic chain in each of the six peripheral positions. Because of the repulsive interactions between ortho protons in the phenylenes and the ones of the neighboring aromatic rings, the phenylenes are likely to be twisted with respect to the HBC core. This loss of planarity of the HBC could play a role in the organization of the molecules when physisorbed into layers at the HOPG−solution interface. In addition, to gain insight into the role of the chirality of the group in the 3′-position, the (*R*,*S*) mixture of **2a**, namely, compound **2b**, and compound **3** have been also analyzed.

The syntheses of alkyl-, and phenylene-alkyl-substituted hexabenzocoronenes, HBC−$C_8$* (**1**) and HBC−$PhC_{12}$ (**3**) respectively, have been previously described in the literature.[15] Here, in the Experimental Section, we will just briefly discuss the synthesis of the optically active HBC−$PhC_8$* (**2a**) and the mixture of stereoisomers HBC−$PhC_8$ (**2b**), which have been synthesized according to similar procedures.

(5) (a) Rabe, J. P.; Buchholz, S. *Science* **1991**, *253*, 424−427. (b) Cyr, D. M.; Venkataraman, B.; Flynn, G. W.; Black, A.; Whitesides, G. M. *J. Phys. Chem.* **1996**, *100*, 13747−13759. (c) Claypool, Ch. L.; Faglioni, F.; Goddard, W. A., III; Gray, H. B.; Lewis, N. S.; Marcus, R. A. *J. Phys. Chem. B* **1997**, *101*, 5978−5995. (d) Samorí, P.; Francke, V.; Müllen, K.; Rabe, J. P. *Chem. Eur. J.* **1999**, *5*, 2312−2317. (e) Stawasz, M. E.; Sampson, D. L.; Parkinson, B. A. *Langmuir* **2000**, *16*, 2326−2342. (f) Qiu, X.; Wang, C.; Zeng, Q.; Xu, B.; Yin, S.; Wang, H.; Xu, S.; Bai, C. *J. Am. Chem. Soc.* **2000**, *122*, 5550−5556. (g) Gesquière, A.; Abdel-Mottaleb, M. M. S.; De Feyter, S.; De Schryver, F. C.; Schoonbeek, F.; van Esch, J.; Kellogg, R. M.; Feringa, B. L.; Calderone, A.; Lazzaroni, R.; Brédas, J. L. *Langmuir* **2000**, *16*, 10385−10391.

(6) (a) Clar, E. *Aromatische Kohlenwasserstoffe: Polycyclische Systeme*; Springer: Berlin, Göttingen, Heidelberg, 1952. (b) Clar, E., *The Aromatic Sextet*; John Wiley: London, 1972. (c) Diederich, F.; Rubin, Y. *Angew. Chem.* **1992**, *104*, 1123−1146; *Angew. Chem., Int. Ed. Engl.* **1992**, *31*, 1101−1123. (d) Faust, R. *Angew. Chem.* **1995**, *107*, 1559−1562; *Angew. Chem., Int. Ed. Engl.* **1995**, *34*, 1429−1432. (e) Hudgins, D. M.; Allamandola, L. J. *J. Phys. Chem.* **1995**, *99*, 3033−3046. (f) Scott, L. T.; Cheng, P.-C.; Hashemi, M. M.; Bratcher, M. S.; Meyer, D. T.; Warren, H. B. *J. Am. Chem. Soc.* **1997**, *119*, 10963−10968. (g) Tong, L.; Lau, H.; Ho, D. M.; Pascal, R. A., Jr. *J. Am. Chem. Soc.* **1998**, *120*, 6000−6006. (h) Debad, J. D.; Bard, A. J. *J. Am. Chem. Soc.* **1998**, *120*, 2476−2477.

(7) (a) Adam, D.; Schuhmacher, P.; Simmerer, J.; Häussling, L.; Siemensmeyer, K.; Etzbach, K. H.; Ringsdorf, H.; Haarer, D. *Nature* **1994**, *371*, 141−143. (b) Simmerer, J.; Glüsen, B.; Paulus, W.; Kettner, A.; Schuhmacher, P.; Adam, D.; Etzbach, K.-H.; Siemensmeyer, K.; Wendorff, J. H.; Ringsdorf, H.; Haarer, D. *Adv. Mater.* **1996**, *8*, 815−819. (c) van de Craats, A. M.; Warman, J. M.; de Haas, M. P.; Adam, D.; Simmerer, J.; Haarer, D.; Schuhmacher, P. *Adv. Mater.* **1996**, *8*, 823−826.

(8) (a) Askadskaya, L.; Boeffel, C.; Rabe, J. P. *Ber. Bunsen-Ges. Phys. Chem.* **1993**, *97*, 517−521. (b) Gabriel, J.-C.; Larsen, N. B.; Larsen, M.; Harrit, N.; Pedersen, J. S.; Schaumburg, K.; Bechgaard, K. *Langmuir* **1996**, *12*, 1690−1692.

(9) Charra, F.; Cousty, J. *Phys. Rev. Lett.* **1998**, *80*, 1682−1685.

(10) Stabel, A.; Herwig, P.; Müllen, K.; Rabe, J. P. *Angew. Chem.* **1995**, *107*, 335−339; *Angew. Chem., Int. Ed. Engl.* **1995**, *34*, 1609−1611.

(11) Goddard, R.; Haenel, M. W.; Herndon, W. C.; Krüger, C.; Zander, M. *J. Am. Chem. Soc.* **1995**, *117*, 30−41.

(12) Herwig, P.; Kayser, C. W.; Müllen, K.; Spiess, H. W. *Adv. Mater.* **1996**, *8*, 510−513.

(13) Müller, M.; Kübel, Ch.; Müllen, K. *Chem. Eur. J.* **1998**, *4*, 2099−2109.

(14) Iyer, V. S.; Yoshimura, K.; Enkelmann, V.; Epsch, R.; Rabe, J. P.; Müllen, K. *Angew. Chem.* **1998**, *110*, 2843−2846; *Angew. Chem., Int. Ed.* **1998**, *37*, 2696−2699.

(15) (a) Fechtenkötter, A.; Saalwächter, K.; Harbison, M. A.; Müllen, K.; Spiess, H. W. *Angew. Chem.* **1999**, *111*, 3224−3228; *Angew. Chem., Int. Ed.* **1999**, *38*, 3039−3042. (b) Fechtenkötter, A.; Tchebotareva, N.; Watson, M.; Müllen, K. *Tetrahedron Symp.* **2001**, *57*, 3769−3783.

(16) van de Craats, A. M.; Warman, J. M.; Fechtenkötter, A.; Brand, J. D.; Harbison, M. A.; Müllen, K. *Adv. Mater.* **1999**, *11*, 1469−1472.

(17) Ito, S.; Wehmeier, M.; Brand, J. D.; Kübel, Ch.; Epsch, R.; Rabe, J. P.; Müllen, K. *Chem. Eur. J.* **2000**, *6*, 4327−4342.

(18) Schmitz-Hübsch, T.; Sellam, F.; Staub, R.; Törker, M.; Fritz, T.; Kübel, Ch.; Müllen, K.; Leo, K. *Surf. Sci.* **2000**, *445*, 358−367.

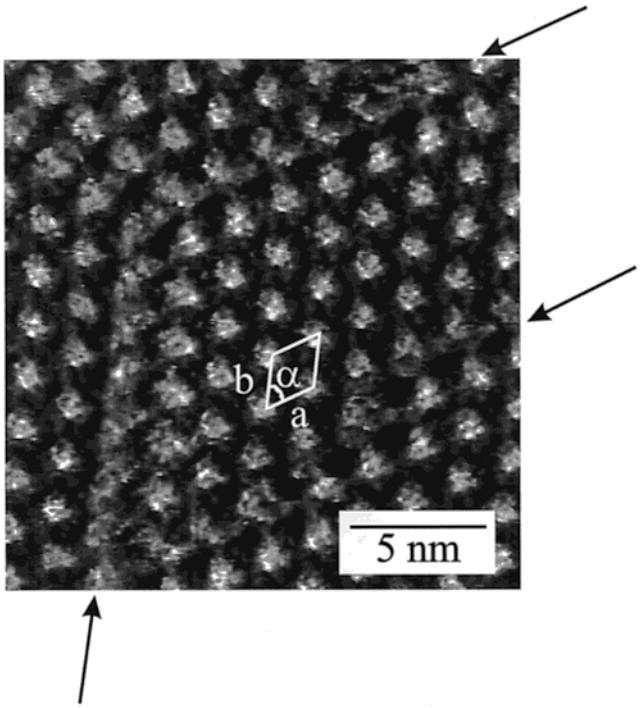


**Figure 2.** Scanning tunneling microscopy current image of **1** at the solution−HOPG interface. The brightness is proportional to the current. The arrows indicate domain boundaries. Unit cell: $a = 1.86 \pm 0.10$ nm; $b = 2.03 \pm 0.10$ nm; $\alpha = 58 \pm 2°$. $U_t = 1.00$ V and average $I_t = 40$ pA.

## Results and Discussion

Figure 2 displays the STM current image of a monolayer of **1** physisorbed at the interface between an organic solution and the basal plane of highly oriented pyrolytic graphite (HOPG). It shows a polycrystalline structure with domain boundaries (indicated by the arrows in Figure 2) that are characterized by a translation of the crystal lattice along one of the three crystallographic axes. Inside each domain, bright spots are arranged (within the experimental error) in a hexagonal motif. These bright spots are attributed to the $\pi$-conjugated cores of the molecules, because in STM current images of alkylated aromatic molecules lying equally flat on HOPG, the aromatic moieties appear brighter (corresponding to higher currents) than the alkyl chains, due to the smaller energy difference between their frontier orbitals and the Fermi level of the substrate.[19] This assignment is consistent with the fact that the area of the unit cell corresponds to the area within the van der Waals contour of a single molecule lying flat on the surface. Since the contrast in STM depends to a great extent also on the spatial overlap of the electronic states of the adsorbate and the substrate, molecules which are placed at variable distances from the substrate can be expected to exhibit different contrasts in the STM current images. Consequently, the distribution of contrasts attained in the STM image in Figure 2 suggests that the aromatic cores are located at equal positions relative to the substrate. The high conformational mobility of the side chains at the surface, which occurs on a time scale faster than the scanning frequency, did not allow us to resolve their structures.

The introduction of a phenylene ring between the aromatic core and the aliphatic side chains in all of the six peripheral positions leads to a dramatic change in the supramolecular structure on the solid surface. Figure 3 displays the STM image

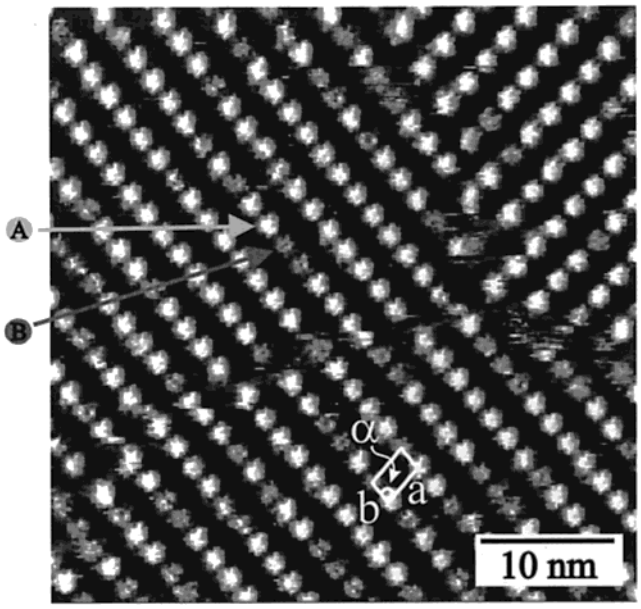


**Figure 3.** Scanning tunneling microscopy current image of **3** at the solution−HOPG interface. An adsorbed molecule with brighter contrast (A) is marked with light gray arrows, while a molecule with darker contrast (B) is labeled in dark gray. Unit cell: $a = 3.10 \pm 0.10$ nm; $b = 2.00 \pm 0.10$ nm; $\alpha = 78 \pm 3°$. $U_t = 1.17$ V; average $I_t = 251$ pA.

of a monolayer of the (*R*,*S*)-phenylene-alkyl-substituted HBC (**3**) physisorbed on HOPG. Similar to the case of **4**, the 2D unit cell of the monolayer is oblique. In contrast to **4**, however, two different types of contrast of the aromatic core have been recorded here, as marked in the image by A (brighter) and B (darker). It is noteworthy that their spatial distribution does not follow a periodical motif. A similar contrast behavior has been observed for the other (*R*,*S*)-phenylene-alkyl functionalized HBC, that is, compound **2b** (image not shown). However, in the latter case, the 2D unit cell is nearly hexagonal ($a = (2.41 \pm 0.12)$ nm; $b = (2.21 \pm 0.12)$ nm; $\alpha = (62 \pm 4)°$).

The STM image of the (*S*)-phenylene-alkyl-substituted HBC derivative, **2a**, self-assembled at the solution−HOPG interface is displayed in Figure 4. Although the 2D packing in the *xy* plane is hexagonal within the experimental error, similar to that of compounds **1** and **2b**, the conjugated cores exhibit three different contrasts distributed in a periodical motif across the plane. In Figure 4, the different cores are marked with A, B, and C, where A exhibits the brightest contrast, and C the lowest. By assuming the unit cell of the aromatic cores marked with I to be exactly hexagonal, molecules exhibiting the same contrast form a $\sqrt{3} \times \sqrt{3}$ R30° superstructure indicated with II.

To quantify the contrasts in the STM current images, the images have been processed. In Figure 4 the average brightness (which corresponds to the mean value of the current determined inside a circle with a diameter of 1.1 nm that has been centered on the middle of the spot) and its standard deviation have been measured for each bright spot. The evolutions of these values along the three lattice axes are plotted versus the position number in Figure 5. In all three profiles in Figure 5, there is a periodicity corresponding to the three neighboring contrasts (A, B, C), although, due to a nonperfect flatness of the image, the absolute values vary across the image. While the long range variations across the whole image are on the order of what is generally observed for more simple crystalline monolayers, for example of **4**, the periodic structure is unique.

The different contrasts, observed in the STM images of the molecules with the phenylene-containing side chains **2a**, **2b,**

(19) Lazzaroni, R.; Calderone, A.; Brédas, J. L.; Rabe, J. P. *J. Chem. Phys.* **1997**, *107*, 99−105.

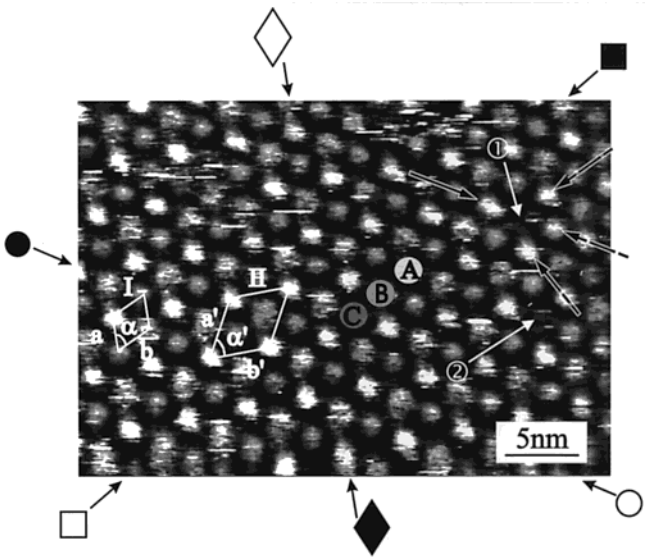


**Figure 4.** Scanning tunneling microscopy current image of **2a** at the solution−HOPG interface. A-, B-, C-types of molecules are characterized by a different contrast. The two white arrows indicate vacancies in the crystal structure. Around the vacancy ① it is possible to notice the presence of three neighboring (labeled dashed black arrow) + one (filled black arrow) A-type of molecules. Unit cell of the 2D structure I: $a = 2.55 \pm 0.10$ nm; $b = 2.44 \pm 0.10$ nm; $\alpha = 58 \pm 3°$. Unit cell of the superstructure II: $a' = 4.28 \pm 0.17$ nm; $b' = 4.28 \pm 0.17$ nm; $\alpha' = 58 \pm 3°$. $U_t = 1$ V; average $I_t = 50$ pA.

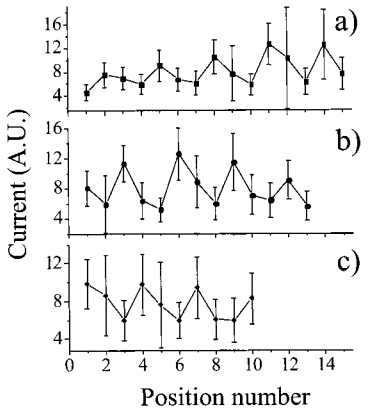


**Figure 5.** Line profiles for the STM image shown in Figure 4. (a) Profile from ■ to □; (b) from ● to ○; (c) from ◆ to ◇. The average spot brightness and its standard deviation are plotted vs the position number, i.e., each unit on the *x*-axis corresponds to one disk. The presented data were obtained by analyzing all pixels in a circular area with a diameter of 1.1 nm centered on the middle of the particular spot.

and **3** (Table 1), could be due to four main effects: (I) defects of the molecular packing on the surface; (II) different number of HBCs in a stack filling the tunneling gap between tip and substrate; (III) different conformation of the molecule; (IV) different position of the molecule in the gap tip−substrate.

The spatially random distribution of two different contrasts for compounds **3** (Figure 3) and **2b** in single crystalline domains physisorbed on HOPG could possibly be explained with effect I, which could be due to: (a) defects in the HOPG lattice or (b) impurities of the molecular material. While (a) can be neglected since the defect density on the freshly cleaved surface of HOPG has been proven with STM to be orders of magnitude smaller, (b) can be ruled out since all of the compounds which have been used are analytically pure (as determined by NMR and mass spectrometry).

**Table 1:** Unit Cell and Contrasts of the Conjugated Cores in the STM Images of Functionalized HBCs

| molecule | unit cell in *xy* | contrasts of the conjugated cores in the STM image |
|---|---|---|
| 1 | hexagonal | 1 contrast |
| 2a | hexagonal | 3 contrasts periodically distributed: "staircase" |
| 2b | hexagonal | 2 contrast randomly distributed |
| 3 | oblique | 2 contrasts randomly distributed |
| 4 | oblique | 1 contrast |

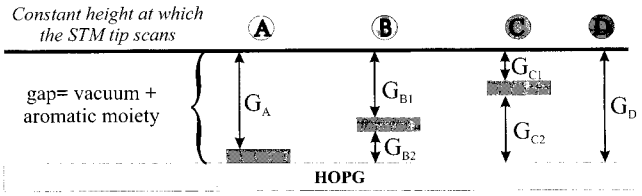


**Figure 6.** Schematic cartoon of STM constant height investigation. The molecule can be localized in different *z* locations within the gap tip−substrate. In all three cases (A,B,C) the size of the not-filled gap, which can be considered as vacuum, is equal: $G_A = G_{B1} + G_{B2} = G_{C1} + G_{C2}$. In the extreme case (D) the gap consists of vacuum where $G_A < G_D$.

Assuming II, the contrast A in Figure 4 could correspond to three stacked disks, B to two, and C to one disk filling the gap tip−substrate, since a stack of aromatic cores should exhibit a better electron transfer than the solvent molecules. However, observing carefully the molecular packing in the proximity of lattice defects such as a missing molecule (indicated with white arrows ① and ② in Figure 4), one can note that these defects are located where one of the darker disks should be placed, albeit it is desorbed. The desorption of a C-type molecule is very unlikely, since among the three types it is the one which is better coupled with the substrate, hence more strongly physisorbed on it. This observation does not support the effect II.

Phenylene groups which are directly attached to the molecular core are common to derivatives **2a**, **2b,** and **3**. To minimize the steric interactions of the ortho protons with those of the neighboring aromatic core, they are likely to arrange in a nonplanar conformation giving rise to a nonplanarity of the whole system.[15a,16] The variation of the conformation (effect III), from planar to nonplanar, can induce a change in the electronic properties of the HBCs, causing different contrasts in the STM current image.

According to interpretation IV, the aromatic cores may be "frozen" at different positions ("staircase") in the tunneling gap tip−substrate, as sketched in the cartoon in Figure 6 In this model, the asymmetric position of the molecule within the gap tip−substrate has an influence on the contrast in STM current images, according to a resonant tunneling contribution.[20] In the case of the STM images of **2a**, which are characterized by three different contrasts, the brighter disks (A) would be better coupled to the substrate, while B and C would appear more and more dark because of their increasing distance from the substrate, and consequently lower coupling (Figure 6). Already a gap shift on the 0.1 nm scale would cause a significant current change.[21] The extreme case would be characterized by the absence of the molecule in the gap (case D), which leads to the smallest current in the STM image, as at vacancies in the 2D lattice (indicated by the white arrows ① and ② in Figure 4). This model is also

(20) Mizutani, W.; Shigeno, M.; Kajimura, K.; Ono, M. *Ultramicrosopy* **1992**, *42*−*44*, 236−241.

(21) Eigler, D.; Lutz, C. P.; Rudge, W. E. *Nature* **1991**, *352*, 600−603.

in accordance with the observation of a missing molecule (white arrows in Figure 4) of type C, which can desorb more easily since it is located further away from the substrate.

We conclude, therefore, that either III or IV, or both of them, cause the different contrast observed in Figures 3 and 4.

The observation that **2a** self-assembles at the solid−liquid interface not only in two dimensions but also with respect to the third dimension is particularly interesting. In addition to the role played by the phenylene groups attached to the molecular core (effect III) inducing a loss of planarity of the whole system, a contribution of the aliphatic side chains for the supramolecular arrangement is likely to be relevant. The branched substitutions themselves, being (*S*), also induce well-defined and periodical losses of planarity. We believe that both of these two chemical functionalities are required to attain the self-assembly into a staircase architecture of **2a**.

On the other hand, the mere existence of the first of the two forces in the case of compound **3**, namely the presence of a phenylene function directly attached to the HBC core, induces a loss of planarity of the system in the nonadsorbed state, that upon physisorption at a surface leads to a molecular pattern with a degree of order only in the *xy* plane, while the molecules are located randomly, that is, in a nonperiodical fashion, in the third dimension in any of two distinct positions. In the absence of the phenylene attached directly to the aromatic core, the molecules tend to physisorb equally flat on the basal plane of graphite, as has also been observed for several other symmetrically functionalized PAHs.[10,14]

Focusing again on the missing molecules in Figure 4, one can notice that the superstructure is lost in their vicinity. For example, a total of four A-type molecules in the vicinity of the vacancy ① in Figure 4 can be recognized: Three neighboring ones are marked with dashed black arrows, and another one is labeled with a filled black arrow. The free space provided by the missing molecule enables the neighboring moieties to attain a position which is more near the substrate if compared to the standard location it would usually assume. This indicates once again that the steric hindrances (intermolecular interactions) are essential to achieve this type of 3D arrangement. Remarkably, these vacancies are rather stable features with a lifetime of several minutes.

A similar supramolecular nanostructure like that of **2a** at the solution−HOPG interface has been detected on triphenylenes bearing long aliphatic side-chains by Charra and Cousty.[9] These authors have observed the appearance of a superlattice in hexagonally packed monolayers with increasing lengths of the side chains, where every third molecule appears brighter, according to a $\sqrt{3} \times \sqrt{3}$ R30° superstructure. They explained this phenomenon in the light of an antiferromagnetic triangular Ising net. However, this model cannot be applied to our data because it cannot be used to describe a structure consisting of more than two contrasts, for example, the staircase built up with **2a**.

Drawing the attention to the symmetry of the molecular arrangement in 2D (Table 1), compounds **1** and **2a** exhibit a 2D hexagonal unit cell, while for **3** it is oblique. In the latter case, the steric hindrance of the nonbranched, that is, linear, aliphatic side chains is smaller, giving rise to a larger flexibility of the molecular system. This may be the reason for **3** to pack according to a two-fold symmetry, similarly to that of HBC−$C_{12}$ (**4**).[10] This packing is favored since the area per unit cell is minimized; hence, the enthalpic gain upon adsorption at the surface (interfacial interaction) is maximized.[22] Instead, in the first three cases **1**, **2a,** and **2b**, due to a larger steric hindrance

**Scheme 1**

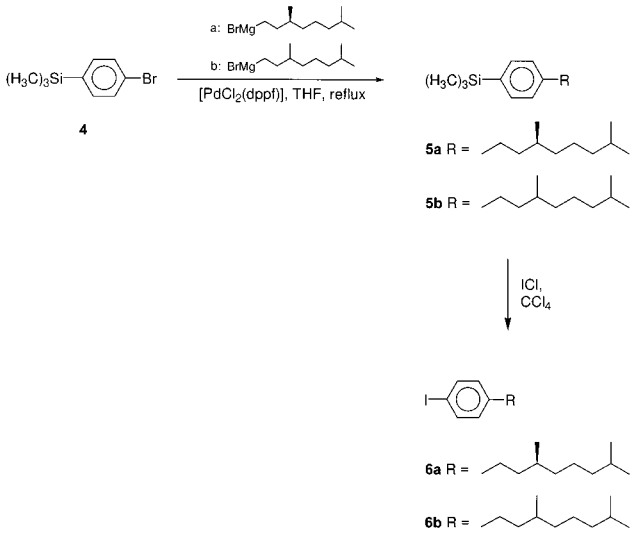


of the nonconjugated bulky peripheral groups, and consequently a smaller flexibility of the system, the HBCs cannot arrange in a two-fold symmetry, thus adopting an almost hexagonal structure, that is reminiscent of columnar mesophases. Indeed, this class of compounds exhibits liquid crystalline phases which exist over a wide range of temperatures.[12,16]

## Conclusions and Outlooks

In summary, the chemical functionalization of HBCs with phenylene-alkyl (*S*) side chains allowed us to extend the established two-dimensional molecular self-assembly at the solid−liquid interface to the third dimension in the region near the substrate. The formation of the staircase architecture finds its origin in the interplay between intramolecular as well as intermolecular and interfacial interactions; a key role is played by the steric hindrance suffered by the side chains. This latter effect can also play a role inducing the molecules to adopt different conformations, allowing the minimization of the intermolecular repulsive interactions. The staircase architecture appears to be an ideal candidate for scanning tunneling spectroscopy studies of equally conjugated molecules possessing different electronic properties due to their variable overlap with the substrate. Furthermore, it is possible to envisage new interesting experiments manipulating a single HBC in the *xy* plane from near-vacancy to vacancy: Depending on the final location that the manipulated molecule spontaneously adopts along the *z* axis, the HBC layer might exhibit properties of a molecular-level machine[23] where the stimulated switch between two different positions with respect to the substrate is controlled by intermolecular interactions.

## Experimental Section

**Synthesis.** The synthesis of compounds **2a** and **2b** is depicted in Schemes 1 and 2. In a first step the commercially available 1-bromo-4-trimethylsilylbenzene (**4**) was alkylated under common Kumada-coupling conditions with an (*S*)- and an (*R*,*S*)-side chain to afford **5a** and **5b**, respectively.[15] The trimethylsilyl-substituted alkyl-benzenes **5a** and **5b** were converted to the iodine-functionalized derivatives **6a** and **6b** via electrophilic substitution[24] using iodine monochloride in carbon

(22) Samorí, P.; Severin, N.; Müllen, K.; Rabe, J. P. *Adv. Mater.* **2000**, *12*, 579−582.
(23) Balzani, V.; Credi, A.; Raymo, F. M.; Stoddart, J. F. *Angew. Chem.* **2000**, *111*, 3484−3530; *Angew. Chem., Int Ed.* **2000**, *39*, 3348−3391.
(24) Wu, R.; Schumm, J. S.; Pearson, D. L.; Tour, J. M. *J. Org. Chem.* **1996**, *61*, 6906−6921.

**Scheme 2**

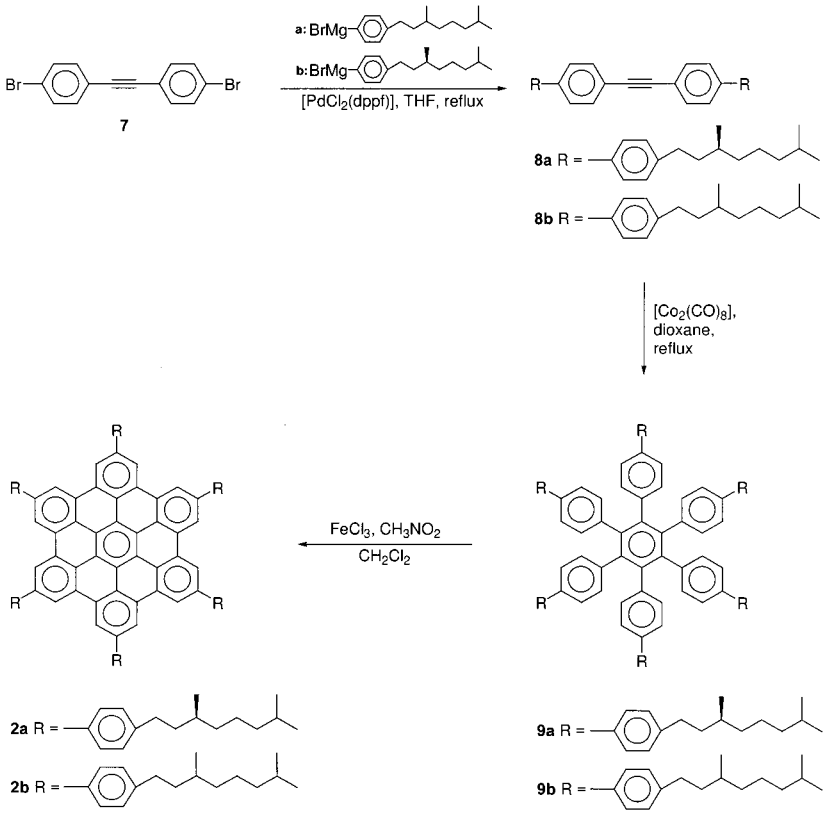


tetrachloride as outlined in Scheme 1. The aryl−aryl coupling of two eqivalents of **6a** or **6b** with 4,4'-dibromodiphenylacetylene (**7**) was carried out under the same conditions described earlier by our group, to yield the (*S*)-bis-biphenyl-4-yl-acetylene **8a** and its (*R*,*S*) derivative **8b** (Scheme 2).[15] In a cyclotrimerization reaction under catalytic the action of $Co_2(CO)_8$ **8a** and **8b** were both transferred to the hexabiphenylylbenzene derivatives **9a** and **9b**, respectively. The cyclodehydrogenation (Scheme 2) was carried out by adding a solution of $FeCl_3$ in nitromethane to the precursors **9a** and **9b** to afford the hexabenzocoronenes **2a** and **2b**. Isolated yields after purification using column chromatography and slow reprecipitation are of the order of 80%.[15]

**STM investigation.** The STM study has been carried out with a home-built beetle-type STM[25] operating at the solid−liquid interface. STM tips have been prepared from a 0.25 mm thick Pt/Ir (80%,20%) wire either by mechanical cutting or by electrochemical etching using a solution of NaCN (6 N) + KOH (2 N). Almost saturated solutions of **1**−**3** (Figure 1) in 1,2,4-trichlorobenzene have been applied to the basal plane of the freshly cleaved highly oriented pyrolitic graphite (HOPG) substrate. The lattice of the underlying HOPG has been visualized during the measurements by simply changing the tunneling parameters; this allowed the calibration of the piezo in the *xy* plane in situ. Unit cells were averaged on several images after their correction for the piezo drift (using SPIP Scanning Probe Image Processor, Version 1.720, Image Metrology ApS, Lyngby, Denmark). STM current images with a submolecular resolution have been recorded using scan rates of ∼20−100 lines/sec. The different contrasts in the STM image of the staircase nanostructure (Figure 4) have been quantified using NIH-Image software (National Institutes of Health, Bethesda, Maryland), selecting manually in the image each bright spot that has been assigned to the conjugated core, and detecting the average gray-scale value and its standard deviation inside a circle with a diameter of 1.1 nm which has been centered on the spot. Profiles of the obtained results are plotted in Figure 5.

(25) Hillner, P. E.; Wolf, J. F.; Rabe, J. P. Humboldt University: Berlin, unpublished results.

**Acknowledgment.** This work was supported by the EU-TMR project SISITOMAS, the Volkswagen-Stiftung (Elektronentransport durch konjugierte molekulare Scheiben und Ketten) and the European Science Foundation through SMARTON.

**Supporting Information Available:** Experimental procedures (PDF). This material is available free of charge via the Internet at http://pubs.acs.org.

JA0111380